THE JOURNAL OF BIOLOGICAL CHEMISTRY VOL. 281, NO. 52, pp. 39796–39805, December 29, 2006

G Protein-coupled Receptor (GPCR) Kinase 2 Regulates Agonist-independent $G_{q/11}$ Signaling from the Mouse Cytomegalovirus GPCR M33*

Received for publication, October 25, 2006 Published, JBC Papers in Press, November 6, 2006, DOI 10.1074/jbc.M610026200

Joseph D. Sherrill and William E. Miller[1]

From the Department of Molecular Genetics, Biochemistry, and Microbiology, University of Cincinnati College of Medicine, Cincinnati, Ohio 45267-0524

The mouse cytomegalovirus M33 protein is highly homologous to mammalian G protein-coupled receptors (GPCRs) yet functions in an agonist-independent manner to activate a number of classical GPCR signal transduction pathways. M33 is functionally similar to the human cytomegalovirus-encoded US28 GPCR in its ability to induce inositol phosphate accumulation, activate NF-κB, and promote smooth muscle cell migration. This ability to promote cellular migration suggests a role for viral GPCRs like M33 in viral dissemination *in vivo*, and accordingly, M33 is required for efficient murine cytomegalovirus replication in the mouse. Although previous studies have identified several M33-induced signaling pathways, little is known regarding the membrane-proximal events involved in signaling and regulation of this receptor. In this study, we used recombinant retroviruses to express M33 in wild-type and $G\alpha_{q/11}{}^{-/-}$ mouse embryonic fibroblasts and show that M33 couples directly to the $G_{q/11}$ signaling pathway to induce high levels of total inositol phosphates in an agonist-independent manner. Our data also show that GRK2 is a potent regulator of M33-induced $G_{q/11}$ signaling through its ability to phosphorylate M33 and sequester $G\alpha_{q/11}$ proteins. Taken together, the results from this study provide the first genetic evidence of a viral GPCR coupling to a specific G protein signaling pathway as well as identify the first viral GPCR to be regulated specifically by both the catalytic activity of the GRK2 kinase domain and the $G\alpha_{q/11}$ binding activity of the GRK2 RH domain.

G protein-coupled receptors (GPCR)[2] represent the largest family of cellular receptors, with over 800 members predicted to be expressed in the human genome (1). GPCRs are present in virtually all free-living organisms and have also been found in numerous viruses including those in the herpesvirus family (2–4). GPCRs are seven-transmembrane domain-spanning proteins that upon agonist binding adopt an active confirmation to stimulate GDP to GTP exchange on the Gα subunit and dissociation from the Gβγ heterodimer. The liberated Gα and Gβγ subunits can then induce a variety of cellular responses through the action of effector proteins and intracellular second messengers. In the case of GPCRs coupled to $G_{q/11}$ proteins, activation of these receptors stimulates phospholipase C-β (PLC-β) activity, resulting in the generation of inositol 1,4,5-triphosphate and diacylglycerol. The concerted action of inositol 1,4,5-triphosphate and diacylglycerol leads to increased levels of intracellular Ca^{2+} and activation of protein kinase C. Although $G_{q/11}$-coupled receptors activate PLC-β via the action of the GTP-bound Gα subunit, $G_{i/o}$-coupled receptors have also been shown to stimulate PLC-β via the action of liberated Gβγ subunits (5, 6).

To regulate the levels of signaling necessary for an appropriate cellular response, activated GPCRs are uncoupled from heterotrimeric G proteins through a process termed desensitization. Desensitization is initiated when activated receptors undergo phosphorylation on serine and threonine residues within the intracellular loops and carboxyl tail by members of the G protein-coupled receptor kinase (GRK) family (7). GRK phosphorylation promotes subsequent binding by β-arrestin proteins, which sterically block G protein coupling, facilitate receptor internalization, and promote G protein-independent, or nontraditional, signaling pathways (7, 8). There are seven members of the GRK family (GRK1–7) that share a highly homologous kinase domain as well as an amino-terminal regulator of G protein signaling (RGS) homology (RH) domain (9). Aside from GRK1 and 7 and GRK4, which are restricted to the retina and testes, respectively, GRKs are ubiquitously expressed and contribute to the phosphorylation and desensitization of most, if not all, activated GPCRs.

GRK2 was one of the first GRK family members identified for its ability to induce phosphorylation of agonist-stimulated β-adrenergic receptor (10). In addition to the RH and catalytic domain, GRK2 contains a carboxyl-terminal pleckstrin homology domain. The pleckstrin homology domain of GRK2 is a phospholipid-binding domain that mediates GRK2 binding to Gβγ, thereby facilitating GRK2 localization to the plasma membrane (11–14). The RH domain of GRK2 is homologous to

* This work was supported by National Institutes of Health Grant R01 AI058159 and March of Dimes Grant 5-FY-04-17. The costs of publication of this article were defrayed in part by the payment of page charges. This article must therefore be hereby marked "*advertisement*" in accordance with 18 U.S.C. Section 1734 solely to indicate this fact.

[1] To whom correspondence should be addressed: Dept. of Molecular Genetics, Biochemistry, and Microbiology, University of Cincinnati College of Medicine, 231 Albert Sabin Way, Cincinnati, OH 45267-0524. Tel.: 513-558-0866; Fax: 513-558-8474; E-mail: william.miller@uc.edu.

[2] The abbreviations used are: GPCR, G protein-coupled receptor; CMV, cytomegalovirus; FACS, fluorescence-activated cell sorting; GFP, green fluorescent protein; GRK, G protein-coupled receptor kinase; HCMV, human cytomegalovirus; HEK, human embryonic kidney; MCMV, mouse cytomegalovirus; MEF, mouse embryonic fibroblast; PNGase F, peptide-*N*-glycosidase F; PLC, phospholipase C; RANTES, regulated upon activation of normal T-cells expressed and secreted; RGS, regulator of G protein signaling; RH, regulator of G protein signaling homology; WT, wild-type; KO, knockout; HA, hemagglutinin.

RGS domains of other proteins, including RGS4, which typically serve as GTPase-activating proteins to promote hydrolysis of GTP to GDP on $G\alpha_{q/11}$ proteins and thereby reduce signaling (15, 16). Interestingly, the RH domain of GRK2 selectively binds GTP-bound $G\alpha_{q/11}$ yet displays little GTPase-activating protein activity. This finding suggests that GRK2 can sequester GTP-bound $G\alpha_{q/11}$ and inhibit GPCR signaling independent of receptor phosphorylation (17, 18). Indeed, a growing list of cellular $G_{q/11}$-coupled receptors have been shown to be regulated by GRK2 through this phosphorylation-independent mechanism, revising the classical paradigm of GRK-mediated GPCR desensitization (17–20).

Cytomegaloviruses (CMVs), members of the betaherpesvirus family, establish lifelong infection in multiple tissues within a restricted host range, inducing characteristic nuclear and cytoplasmic inclusions within infected cells (21). Cytomegalovirus infection is typically asymptomatic within the healthy host; however, congenital CMV infection or infection of immunocompromised hosts can result in a variety of disease syndromes including mental retardation, retinitis, and rejection of transplanted organs (21).

Recently, GPCR homologs have been identified within the genomes of several herpesviruses including CMV. These virally encoded GPCRs are speculated to have been "pirated" from the genome of the infected host throughout the evolution of the virus to alter host cell signaling pathways for the benefit of viral replication, dissemination, and/or immune evasion (22). The mouse cytomegalovirus (MCMV) encodes two GPCRs, M33 and M78, which, based on genome organization, are homologs of the human cytomegalovirus (HCMV) GPCRs UL33 and UL78, respectively (23, 24). Although M33 appears to be homologous to UL33, it retains signaling properties more similar to that of another HCMV GPCR termed US28 (25). Early studies showed that M33 and US28 signal in an agonist-independent manner to induce accumulation of inositol phosphates, suggesting that US28 and M33 can couple to the $G_{q/11}$ signaling pathway (26). Additionally, both US28 and M33 were shown to stimulate the transcriptional activity of NF-κB and CREB *in vitro* (26). More recently, data have suggested that US28 and M33 could promote smooth muscle cell migration, an early event in the formation of arterial plaques and the development of atherosclerosis (27, 28). In addition to the potential role of these viral GPCRs in the development of atherosclerosis, the ability of CMV GPCRs to stimulate cellular migration may have broader implications during viral replication *in vivo* and may contribute to viral dissemination or pathogenesis.

Because of the strict species specificity of CMV, no *in vivo* model is available to study the role of US28 in HCMV pathogenesis. However, the importance of M33 in MCMV pathogenesis was emphasized in studies where recombinant MCMV deleted for M33 displayed decreased viral dissemination to and replication within the salivary gland *in vivo* (29). The parallels in activated intracellular signaling pathways between M33 and US28 suggest that the latter may play a similar role in HCMV pathogenesis *in vivo*. In the present study, we sought to determine the membrane-proximal events involved in M33 signaling and regulation. We utilized mouse embryonic fibroblasts (MEFs) from wild-type and $G\alpha_{q/11}$ knock-out animals to demonstrate that M33 directly couples to the $G_{q/11}$ signaling pathway to stimulate inositol phosphate accumulation in an agonist-independent manner. Additionally, we have identified M33 as the first viral GPCR to be regulated by both the catalytic and RH domains of GRK2. Taken together, our data suggest that although M33 retains the characteristic agonist-independent signaling activity observed from other viral GPCRs such as US28, it is dually regulated by GRK2 similar to various host cell $G_{q/11}$-coupled receptors.

EXPERIMENTAL PROCEDURES

Cell Lines and Transfection—Human embryonic kidney (HEK) 293 cells and HEK293T cells were obtained from the American Type Culture Collection (CRL-1573 and CRL-11268, respectively) and maintained at 37 °C in 5% CO_2 in minimal essential medium supplemented with 10% fetal bovine serum and penicillin-streptomycin. Wild-type (WT) and $G\alpha_{q/11}$ knock-out (KO) MEFs were kindly provided by Dr. S. Offermanns (University of Heidelberg, Heidelberg, Germany) and maintained at 37 °C in 5% CO_2 in Dulbecco's modified essential medium supplemented with 10% fetal bovine serum and penicillin-streptomycin (30). For all of the transient transfections, the cells were transfected using Mirus *Trans*-IT® LT-1 according to the manufacturer's instructions (Mirus Bio Corp.).

Plasmids—The M33 cDNA was cloned from DNA isolated from NIH3T3 cells infected with the MCMV strain $K181^+$ (kind gift from Dr. R. Cardin, Children's Hospital Medical Center, Cincinnati, Ohio) and inserted into the EcoRV site within the mammalian expression vector pcDNA3 (Invitrogen). M33HA and M33FLAG were created by PCR from M33 cDNA using a 3′ oligonucleotide encoding for the HA epitope (YPYDVPDYA) or FLAG epitope (DYKDDDDK), respectively. The resulting M33HA and M33FLAG sequences were cloned into the HindIII and XhoI restriction sites of pcDNA3 and verified by DNA sequencing. M33ΔN, an M33 amino-terminal deletion mutant lacking the first 10 predicted amino acids, was cloned from pcDNA3-M33 using the 5′ oligonucleotide 5′-GCGGATCCGGACCATGGACGAGAGCGACTACCTG-3′ and inserted into the BamHI and EcoRI sites in pcDNA3. M33ΔNFLAG was created similarly to M33FLAG, using pcDNA3-M33ΔN as a template. M33-R131A was generated from pcDNA3-M33 by a two-step PCR method using overlapping oligonucleotides encoding GCG at base pairs 391–393 in the M33 cDNA. The two PCR products were then used as templates in another round of PCR to generate M33-R131A, which was inserted into pcDNA3 and verified by DNA sequencing. M33HA-R131A was created by PCR from pcDNA3-M33-R131A using the same 3′ oligonucleotide used to generate M33HA. All untagged GRK2 constructs cloned into pcDNA3, as well as the Myc-tagged GRK2 and GRK2 D110A constructs, were kindly provided by Drs. R. Sterne-Marr ((Siena College, Loudonville, NY) and S. Ferguson (The University of Western Ontario, London, Ontario, Canada). The Myc-tagged GRK2 K220R and K220R/D110A constructs were generated by restriction digest of the parental plasmid at the KpnI sites within the GRK2 cDNA and pcDNA3. Fragments were then ligated into the KpnI site in pcDNA3 MycGRK2 or MycGRK2 D110A, respectively, and correct insert orientation was verified by DNA sequencing. For fluorescent confocal microscopy

experiments, M33 and M33ΔN cDNAs were cloned in frame into the EcoRI and XhoI sites within the multiple cloning site of pEGFPN-2 (Clontech).

Fluorescent Microscopy—HEK293 cells were plated onto collagen-coated 25-mm glass coverslips and transfected with 1.0 μg of pEGFPN-2, pEGFPN-2 M33 (M33GFP) or pEGFPN-2 M33ΔN (M33ΔNGFP). Forty-eight hours post-transfection, the cells were visualized using a Zeiss 510 inverted confocal microscope.

Inositol Phosphate Accumulation Assay—Transiently transfected HEK293 cells or retrovirally transduced MEFs were radiolabeled with 1.0 μCi/ml [^{3}H]myoinositol overnight. The cells were then treated with 20 mM LiCl for 3 h, after which cell lysates were prepared in 0.4 M perchloric acid and neutralized in 0.72 M KOH and 0.6 M $KHCO_3$. For AlF_4^- stimulation of Gα proteins, the cells were treated with 20 μM $AlCl_3$ and 20 mM NaF during LiCl incubation, and lysates were prepared in a similar manner as described above. The lysates were then applied to Dowex columns (AG1-X8; Bio-Rad), washed, and eluted in 0.1 M formic acid and 1 M ammonium formate. The eluates were counted in a liquid scintillation counter and corrected for total [^{3}H]myoinositol incorporation. The data were analyzed using GraphPad Prism 4 software and presented as fold inositol phosphate accumulation over basal.

Co-immunoprecipitations and Western Blot—Forty-eight hours after transfection, HEK293 cell lysates were prepared in 1.0 ml of Nonidet P-40 lysis buffer (50 mM HEPES, 0.5% Nonidet P-40, 250 mM NaCl, 10% glycerol, 2 mM EDTA, 1 mM phenylmethylsulfonyl fluoride, 2.5 μg/ml aprotinin, 5.0 μg/ml leupeptin, 100 μM sodium orthovanadate, and 1 mM sodium fluoride). The cell lysates were precleared by incubating with 50 μl of glutathione-Sepharose® beads (Amersham Biosciences) and tumbling for 30 min at 4 °C. The lysates were then incubated with 50 μl of anti-FLAG® M2-agarose beads (Sigma), anti-HA.11-Sepharose beads (Covance), or anti-Myc agarose beads (Sigma) and tumbled for 3 h at 4 °C. Immunoprecipitated complexes were washed three times with lysis buffer and then solubilized in 3× Laemmli sample buffer. The samples were then subjected to SDS-PAGE, transferred to nitrocellulose membranes, and blotted with primary anti-HA (1:2000) (Santa Cruz), anti-Myc (1:2000) (Sigma), or anti-$G\alpha_{q/11}$ (1:1000) antibodies (Santa Cruz). Horseradish peroxidase-conjugated anti-rabbit IgG secondary antibodies (1:5000) (Amersham Biosciences) and enhanced chemiluminescence were used for detection and visualization of immunoprecipitating proteins, respectively.

Receptor Deglycosylation—Forty-eight hours post-transfection, HEK293T cells expressing M33FLAG or M33ΔNFLAG were washed with phosphate-buffered saline and lysed in denaturing buffer (0.5% SDS, 1% 2-mercaptoethanol). The lysates were passed through a 22-gauge needle, briefly sonicated, and cellular debris was pelleted at 15,000 rpm for 5 min. The supernatants were then boiled at 100 °C for 5 min, cooled, and Nonidet P-40 was added to a final concentration of 0.75%. The samples were then untreated or treated with 500 units of PNGase F (New England BioLabs) for 30-s, 5-min, and 15-min time intervals. The samples were then subjected to Western blotting with anti-FLAG antibodies (1:1,000; Santa Cruz) as described above.

Fluorescence-activated Cell Sorting (FACS)—Forty-eight hours after transduction, WT and $G\alpha_{q/11}$ KO MEFs were trypsinized and FACS analyzed using the BD FACSCalibur system (BD Biosciences). The data from three independent experiments performed in duplicate were analyzed using CellQuest software, and representative histograms are presented.

Retroviral Production and Transduction—M33 cDNA was blunt cloned into the HpaI site within the MigR1 retroviral vector to generate MigR1-M33. MigR1 is a bicistronic retroviral vector containing a multiple cloning site upstream of an internal ribosome entry site followed by the cDNA encoding for enhanced green fluorescent protein (GFP) (31). MigR1 or MigR1-M33 (3 μg) was then transiently co-transfected with 1 μg of pVSV-G into the packaging cell line HEK GP2–293 (Clontech). Supernatants containing VSV-G pseudotyped MigR1 or MigR1-M33 retroviruses were collected at 48 and 72 h post-transfection. For transduction of WT and $G\alpha_{q/11}$ KO MEFs, 1×10^5 cells were plated in 12-well plates, and twenty-four hours later appropriate amounts of MigR1 or MigR1-M33 supernatants were added to the media. The 12-well plates were then centrifuged at 1800 rpm for 45 minutes at room temperature to facilitate viral binding. Forty-eight hours after infection, the cells were assayed by FACS or inositol phosphate accumulation assay as described.

In Vivo Kinase Assay—Forty-eight hours after transfection, HEK293 cells were washed and incubated in phosphate-free Dulbecco's modified essential medium for 30 min. The cells were then labeled with 500 μCi/ml [^{32}P]H_3PO_4 (MP Biomedicals) for 3 h, washed with cold phosphate-buffered saline, and lysed in 1.0 ml of Nonidet P-40 lysis buffer for 20 min at 4 °C. The cell lysates were precleared by incubating with 50 μl of glutathione-Sepharose® beads and tumbling for 30 min at 4 °C. The lysates were then incubated with 50 μl of anti-FLAG® M2-agarose beads and tumbled for 3 h at 4 °C. Immunoprecipitated complexes were washed three times with lysis buffer and then solubilized in 3× Laemmli sample buffer. The samples were then subjected to SDS-PAGE and autoradiography. M33FLAG phosphorylation was analyzed by ImageQuant software, and the data were plotted using GraphPad Prism 4 software.

RESULTS

The M33 Amino Terminus and NRY Motif Are Required for Stimulation of Inositol Phosphate Accumulation—In this study we investigated the G protein coupling and GRK regulation employed by the viral M33 GPCR during signal transduction. M33 was cloned from NIH3T3 cells infected with the K181$^+$ strain of MCMV and inserted into the eukaryotic expression vector pcDNA3. Similar to other members of the UL33 family, M33 has been predicted to contain an alternative start site in the amino terminus, generating a truncated transcript lacking the first 10 amino acids (29). An expression construct for this truncated M33 protein (termed M33ΔN) was similarly cloned into pcDNA3. To assess signaling of M33, HEK293 cells were transiently transfected with pcDNA3 (mock) or increasing amounts of M33 (0.01, 0.05, 0.25, and 1.25 μg), and inositol phosphate accumulation was assessed. HEK293 cells transfected with M33 showed a dose-dependent increase in inositol phosphates measured in the absence of agonist in agreement

with previous studies using full-length M33 in COS-7 cells (Fig. 1*A*). Similar signaling activity was observed with carboxyl-terminal epitope-tagged versions of M33 (data not shown). Previous reports indicated that M33-mediated stimulation of smooth muscle cell migration was enhanced in the presence of the β-chemokine RANTES, suggesting that M33 signaling could be facilitated by agonist (28). However, we observed no significant increase in M33-induced inositol phosphate accumulation in the presence of up to 500 ng/ml of mouse RANTES (data not shown), further supporting the idea that M33 signals in an agonist-independent manner.

To assess the signaling activity of M33ΔN, which lacks the first 10 amino acids of M33, we analyzed the ability of this truncated protein to stimulate inositol phosphate accumulation. As shown in Fig. 1*B*, M33ΔN fails to induce the formation of inositol phosphates as compared with full-length M33. To determine whether this loss in signaling activity is due to a defect in the ability of M33ΔN to properly localize to the plasma membrane, HEK293 cells were transfected with empty pEGFP-N2 vector (mock), GFP-tagged M33 (M33GFP), or GFP-tagged M33ΔN (M33ΔNGFP) and visualized using fluorescent confocal microscopy. In Fig. 1*C*, mock transfected cells expressing GFP alone displayed a diffuse cytoplasmic and nuclear staining of GFP (*left panel*), whereas cells transfected with M33GFP show prominent expression of M33 at the cell surface (*middle panel*). In contrast, cells transfected with M33ΔNGFP displayed little or no cell surface expression with the majority of localization within the cytoplasm (*right panel*).

The altered membrane localization of M33ΔN suggests that deletion of the 10 amino-terminal residues in M33 prevents proper maturation and trafficking to the plasma membrane. Post-translational modifications, such as glycosylation, have shown to occur on both cellular and viral GPCRs (32, 33). Because M33 has been predicted to contain a consensus *N*-linked glycosylation site at Asn^{20} (29), we sought to determine the glycosylation state of full-length M33 and the amino-terminal deletion mutant M33ΔN. Extracts from HEK293T cells expressing M33FLAG or M33ΔNFLAG were treated with the glycosidase PNGase F, and changes in molecular mass were monitored by Western blot with anti-FLAG antibodies (Fig. 1*D*). In untreated extracts from cells expressing full-length M33FLAG, M33 runs as a broad series of bands, each with a molecular mass of ~45 kDa; however, after 15 min of treatment with PNGase F, M33 runs as a single faster migrating band of ~35 kDa. This result indicates that wild-type M33 is a mature glycosylated protein. Conversely, no shift in molecular mass is observed following PNGase F treatment of extracts from cells expressing M33ΔN, indicating that M33ΔN fails to undergo glycosylation. Taken together with the confocal data, our results suggest that the amino terminus of M33 is necessary for proper maturation and subsequent membrane localization of the receptor. Based on these observations, full-length M33 constructs containing the 10 amino-terminal residues were utilized for the following experiments in this study.

Cellular GPCRs contain specific motifs necessary for G protein coupling. The DRY (Asp-Arg-Tyr) motif, a conserved feature located between the third transmembrane domain and the second intracellular loop, has been shown to be essential for G

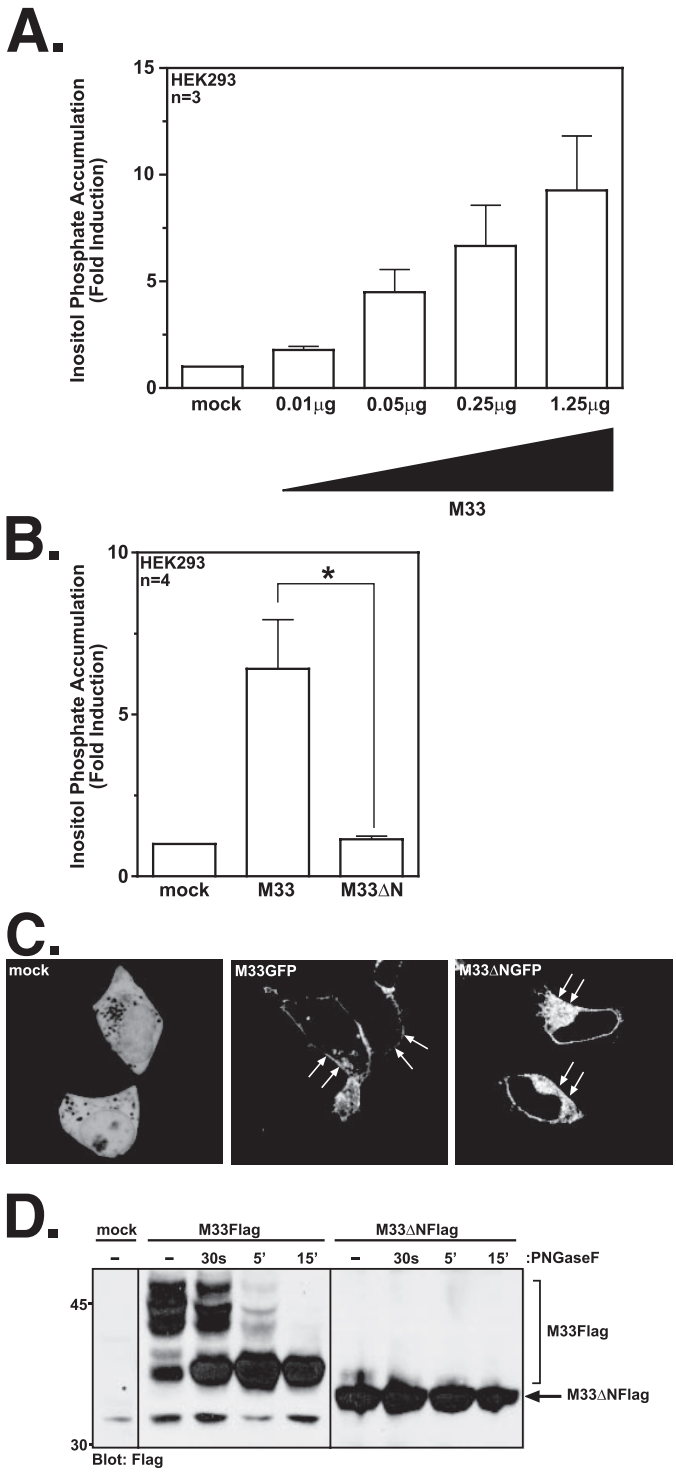

FIGURE 1. **The amino terminus of M33 is required for stimulation of inositol phosphate accumulation.** *A*, HEK293 cells were transfected with pcDNA3 (mock) or increasing amounts of M33 (0.01, 0.05, 0.25, and 1.25 μg) and subjected to an inositol phosphate accumulation assay. The data represent three independent experiments performed in triplicate. *B*, HEK293 cells were transfected with pcDNA3 (mock), M33 (1.25 μg), or M33ΔN (1.25 μg) and subjected to an inositol phosphate accumulation assay. The data represent four independent experiments performed in triplicate (*, $p < 0.05$). *C*, HEK293 cells transfected with pEGFN-2 (mock), M33GFP (1.0 μg), or M33ΔNGFP (1.0 μg) were visualized by fluorescent confocal microscopy. *D*, lysates from HEK293T cells transiently transfected with pcDNA3 (mock), M33FLAG, or M33ΔNFLAG were treated with PNGase F for 30 s, 5 min, or 15 min. The effects of PNGase on promoting deglycosylation of M33 proteins was assessed by Western blot using anti-FLAG antibodies.

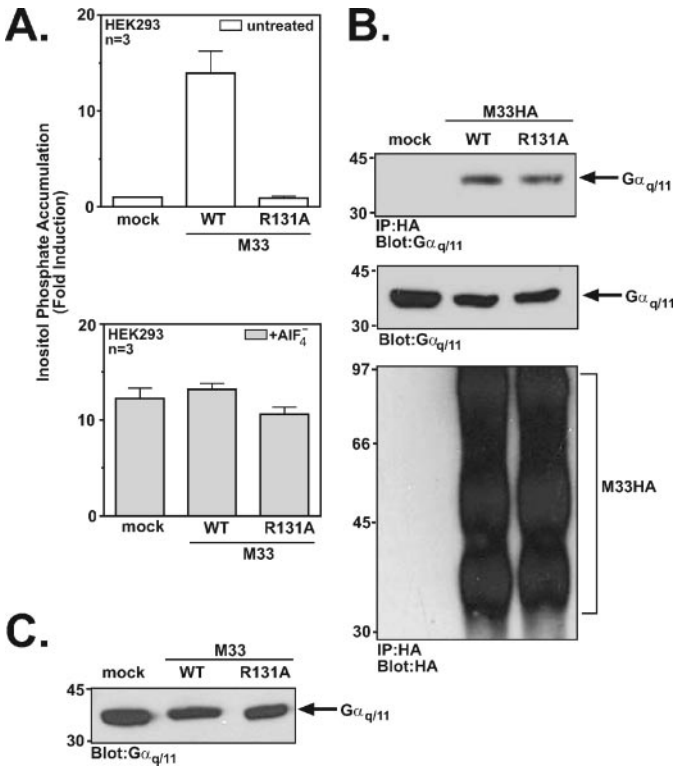

FIGURE 2. **The NRY motif of M33 is required for inositol phosphate signaling; a potential role for $G\alpha_{q/11}$ proteins.** *A*, untreated (*upper panel*) or AlF_4^--treated (*lower panel*) HEK293 cells transfected with pcDNA3 (mock), WT M33 (1.25 μg), or M33-R131A (1.25 μg) were subjected to an inositol phosphate accumulation assay. The data represent three independent experiments performed in triplicate. *B*, HEK293 cells were transfected with pcDNA3 (mock), M33HA (2.0 μg), or M33HA-R131A (2.0 μg) and $G\alpha_q$ (2.0 μg). M33 was immunoprecipitated (*IP*) from cell lysates with anti-HA conjugated agarose beads, and associated $G\alpha_q$ was detected by immunoblot (*upper panel*). Total $G\alpha_q$ in cell lysates was detected by immunoblot (*middle panel*). Immunoprecipitating M33HA and M33HA-R131A were detected by immunoblotting with anti-HA antibodies (*lower panel*). *C*, an immunoblot showing equivalent amounts of endogenous $G\alpha_{q/11}$ proteins from mock, WT M33, and M33-R131A-transfected cells from Fig. 2*A* is shown.

protein coupling and signaling activity (34). However, many constitutively active GPCRs, including mutant cellular GPCRs and those encoded by herpesviruses, have been shown to contain other amino acids within the DRY motif, which appear to promote agonist-independent G protein signaling activity (35–38). In the case of M33, the Asp of the conserved DRY motif is replaced with an Asn, creating a NRY motif. To test the significance of this motif in M33 signaling activity, we replaced Arg^{131} with Ala to create M33-R131A and compared inositol phosphate accumulation with wild-type M33 in HEK293 cells. As shown in Fig. 2*A* (*upper panel*), M33-R131A is defective in its ability to generate inositol phosphates compared with wild-type M33 (~0.89-fold *versus* 13.9-fold, respectively). These data suggest that M33 requires a functional NRY motif to induce inositol phosphate accumulation and that, similar to cellular GPCRs, M33 actively couples to host cell G proteins for signaling activity.

Cellular GPCRs capable of inducing inositol phosphate accumulation have been shown to be coupled either to $G_{q/11}$ (mediated by GTP-bound $G\alpha$ subunits) or $G_{i/o}$ (mediated by liberated $G\beta\gamma$ subunits) signaling pathways (5, 6). To begin to determine the pathway to which M33 is coupled and to determine whether M33 does in fact interact with cellular G proteins, we performed co-immunoprecipitation studies in HEK293 cells co-transfected with epitope-tagged M33HA or M33HA-R131A and $G\alpha_q$. We observed strong interaction between M33 and $G\alpha_q$, suggesting that M33 directly interacts with heterotrimeric G proteins of the $G_{q/11}$ class (Fig. 2*B*). This interaction was also observed between $G\alpha_q$ and the M33-R131A mutant, indicating that although Arg^{131} in the M33 NRY motif is required for induction of inositol phosphate accumulation (Fig. 2*A*), it is not required for interaction with G proteins. To further explore the inability of M33-R131A to induce inositol phosphate accumulation, we used AlF_4^- to directly activate G proteins coupled to phospholipase C in cells transfected with empty vector, M33-WT or M33-R131A. AlF_4^- directly binds $G\alpha$ subunits, and the resulting $G\alpha$-GDP-AlF_4^- assumes an active conformation resembling that of $G\alpha$-GTP (39–41). We observed similar levels of AlF_4^--stimulated inositol phosphate accumulation in all three cell types demonstrating that the lack of signaling in M33-R131A expressing cells is not due to defective G protein-dependent signaling (Fig. 2*A*, *lower panel*). Moreover, Western blot analysis demonstrates that endogenous $G_{q/11}$ expression is equivalent in all cell types (Fig. 2*C*). Taken together, these results indicate that the ability to activate G proteins and stimulate downstream signaling events is uncompromised in cells expressing M33-R131A. Thus, we can infer that the failure of M33-R131A to induce inositol phosphate accumulation is due to an inability to productively engage G proteins. This is consistent with structural and functional studies suggesting that the Arg residue within the DRY motif of other GPCRs is important in stabilizing receptor conformation, and thus GDP to GTP exchange on $G\alpha$ subunits, rather than facilitating G protein interaction (34, 42).

$G\alpha_{q/11}$ Proteins Are Required for M33-stimulated Inositol Phosphate Accumulation—Our data with the inositol phosphate accumulation and $G\alpha_q$ co-immunoprecipitation experiments suggest that M33 couples to the $G_{q/11}$ pathway to induce inositol phosphate accumulation. However, there remains a lack of genetic evidence supporting this hypothesis. Additionally, stimulation of PLC-β by liberated $G\beta\gamma$ dimers from activated $G_{i/o}$-coupled GPCRs has been observed and cannot be excluded for M33 (5). To show that M33-induced inositol phosphate accumulation is mediated through $G_{q/11}$ proteins, we generated a recombinant retrovirus expressing M33 and assessed inositol phosphate accumulation in WT or $G\alpha_{q/11}$ KO MEFs. We have utilized MigR1-based retroviruses in these experiments because MigR1 also expresses GFP on a bicistronic mRNA and enables us to assess transduction efficiency using GFP as a marker. Transduction efficiencies of WT and KO MEFs infected with MigR1 or MigR1-M33 viruses were analyzed for GFP expression by FACS and demonstrated to be similar (Fig. 3*A*). Transduced cells were then assayed for inositol phosphate accumulation (Fig. 3*B*). WT MEFs transduced with MigR1-M33 exhibited high levels of inositol phosphate accumulation compared with MigR1-transduced cells. This effect of M33 was absent in similarly transduced $G\alpha_{q/11}$ KO MEFs, indicating that the $G_{q/11}$ pathway is required for M33-stimulated inositol phosphate accumulation. This is the first genetic evidence directly linking a virally encoded GPCR cou-

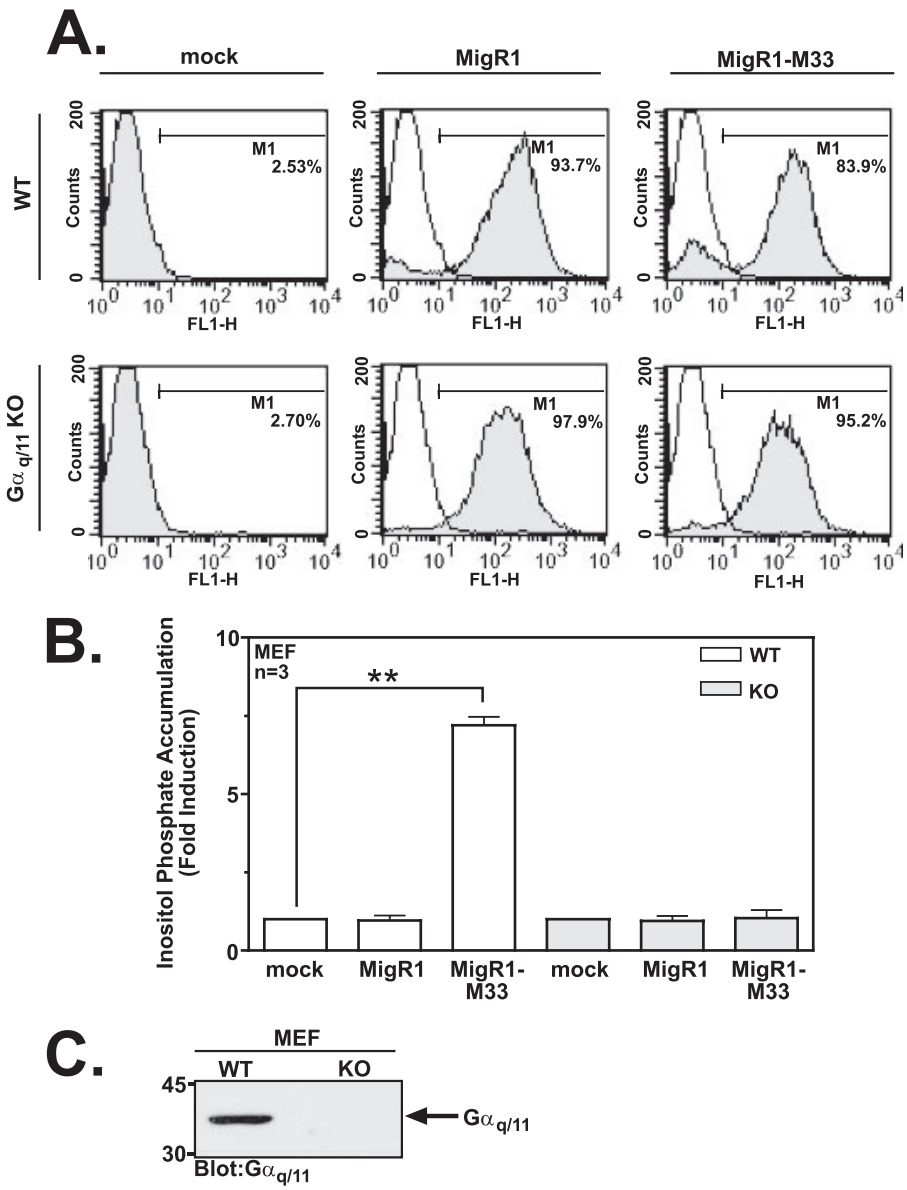

FIGURE 3. **M33 couples directly to $G\alpha_{q/11}$ to stimulate inositol phosphate accumulation.** *A*, WT and $G\alpha_{q/11}$ KO MEFs were untreated (mock) or transduced with MigR1 or MigR1-M33 retroviruses and analyzed for GFP expression by FACS. The data shown are representative of three independent experiments. *B*, mock treated or transduced WT (*open bars*) and $G\alpha_{q/11}$ KO (*shaded bars*) MEFs were subjected to an inositol phosphate accumulation assay. The data represent three independent experiments performed in duplicate (**, $p < 0.005$). *C*, equivalent amounts of WT and $G\alpha_{q/11}$ KO MEFs whole cell lysates were immunoblotted for expression levels of $G\alpha_{q/11}$.

pling to a specific G protein signaling pathway. To confirm the absence of $G\alpha_{q/11}$ expression levels in the $G\alpha_{q/11}$ KO MEFs, equivalent protein extracts from WT and $G\alpha_{q/11}$ KO MEFs were immunoblotted with polyclonal antibodies recognizing both $G\alpha_q$ and $G\alpha_{11}$ proteins (Fig. 3*C*). As expected, WT MEFs, but not $G\alpha_{q/11}$ KO MEFs, express endogenous $G\alpha_{q/11}$ proteins.

GRK2 Regulation of M33 $G_{q/11}$ Signaling Requires Both the GRK2 RH and Catalytic Domains—GRKs play an important regulatory role in GPCR signaling by dampening the response of an activated receptor. This desensitization is necessary for an appropriate level of cellular response and is often initiated by GRK-mediated phosphorylation of the activated receptor. However, a number of $G_{q/11}$-coupled GPCRs regulated by GRKs, specifically GRK2, have been shown to be regulated through both phosphorylation-dependent and phosphorylation-independent mechanisms (18, 20, 43, 44). GRK2 contains an amino-terminal RH domain, a central kinase (CAT) domain, and a carboxyl-terminal pleckstrin homology domain (Fig. 4*A*). Previous studies have shown that a D110A point mutation within the RH domain abrogates GRK2 sequestration of activated GTP-bound $G\alpha_{q/11}$ (45). Similarly, a K220R point mutation within the kinase domain inhibits GRK2 catalytic activity (46). To determine whether GRK2 regulates M33-induced formation of inositol phosphates and to investigate the contribution of the GRK2 RH and kinase domains, HEK293 cells were co-transfected with pcDNA3 (mock) or M33 and WT GRK2 (Fig. 4*B*). In the absence of exogenous GRK2, M33 induces high levels of inositol phosphate accumulation compared with mock treated cells (~14-fold over basal). This induction, however, is significantly attenuated when GRK2 is co-expressed, suggesting GRK2 regulates M33 coupling to the $G_{q/11}$ pathway. Interestingly, when co-expressed with the D110A or K220R point mutants, M33-induced inositol phosphate accumulation was also significantly diminished, although not to the same degree as observed with WT GRK2. In contrast, the D110A/K220R mutant (which exhibits no RH or kinase activity) was completely defective in its ability to attenuate M33 signaling. These data indicate that regulation of M33 signaling through the $G_{q/11}$ pathway is dependent on both the catalytic activity of the GRK2 kinase domain and the $G\alpha_{q/11}$ binding activity of the GRK2 RH domain.

GRK2 Interacts with and Phosphorylates M33—To ensure that the effects of the various GRK2 point mutants on M33 signaling are not due to defects in interactions with M33, we performed co-immunoprecipitation studies in HEK293 cells transfected with pcDNA3 (mock) or M33FLAG co-expressed with Myc-tagged WT GRK2, GRK2 D110A, GRK2 K220R, or GRK2 D110A/K220R. As shown in Fig. 5*A*, each of the GRK2 mutants interacted with M33 to similar levels, suggesting that our results in Fig. 4*B* are not due to altered GRK2 interaction with M33.

As suggested in the results from Fig. 4*B*, the catalytic activity of the GRK2 kinase domain appears to play an important role in

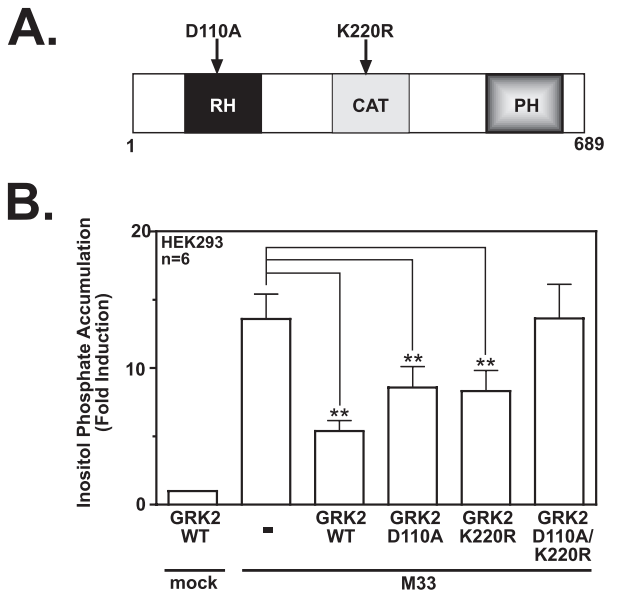

FIGURE 4. **GRK2 regulation of M33 $G_{q/11}$ signaling requires the GRK2 RH and catalytic domains.** *A*, a schematic of the structure of GRK2 shows the RH, kinase (CAT), and pleckstrin homology domains. Highlighted are the D110A and K220R point mutations within the RH and kinase domains, respectively. *B*, HEK293 cells were transfected with pcDNA3 (mock) or M33 (1.25 μg) and WT GRK2, D110A, K220R, or D110A/K220R (1.25 μg) and subjected to an inositol phosphate accumulation assay. The data represent six independent experiments performed in triplicate (**, $p < 0.005$).

the regulation of M33 signaling. To determine whether GRK2 phosphorylation of M33 plays a role in the regulation of signaling, we performed *in vivo* kinase assays in HEK293 cells expressing M33 and WT GRK2, GRK2 D110A, or GRK2 K220R (Fig. 5*B*, *upper panel*). When expressed alone in HEK293 cells, M33 displays a basal amount of phosphorylation, potentially resulting from endogenous GRKs or from other endogenous cellular kinases. This basal phosphorylation state is significantly increased when M33 is co-expressed with either WT GRK2 or the D110A mutant by 51 and 69%, respectively (Fig. 5, *B* and *C*). However, this increase is not observed when M33 is co-expressed with the catalytically inactive K220R point mutant. These results show that catalytically active GRK2 phosphorylates M33 and suggest that this increase in the phospho-content of the receptor leads to the attenuated M33 signaling observed in Fig. 4*B*.

GRK2 Sequestration of $G\alpha_{q/11}$ Requires a Functional RH Domain—Previous studies have shown that the RH domain of GRK2 specifically interacts with activated GTP-bound $G\alpha_{q/11}$, but not GDP-bound $G\alpha_{q/11}$ (17, 18). This interaction is thought to result in GRK2-mediated phosphorylation-independent regulation of $G_{q/11}$-coupled GPCRs by preventing $G\alpha_{q/11}$ from interacting with PLC-β. To illustrate the importance of the RH domain of GRK2 in binding $G\alpha_{q/11}$, we performed co-immunoprecipitation studies in HEK293 cells transfected with pcDNA3 (mock) or either Myc-tagged WT GRK2, D110A, K220R, or D110A/K220R, and $G\alpha_q$. As shown in Fig. 6, $G\alpha_q$ co-immunoprecipitated with WT GRK2 and the K220R point mutant, but not the D110A or D110A/K220R point mutants. These data confirm previous reports identifying the RH domain of GRK2 as necessary for the sequestration of activated GTP-bound $G\alpha_{q/11}$.

Schematic of M33 Signaling and Desensitization—Given the data presented in this study, we have developed the following model for M33 signaling and regulation (Fig. 7). MCMV infection of a host cell leads to expression of M33, which localizes at the plasma membrane (Fig. 7*A*, *inset*). Once expressed at the cell surface, M33 induces high levels of inositol phosphate accumulation in an agonist-independent manner through coupling to the $G_{q/11}$ family of heterotrimeric G proteins. Our data suggest that GRK2 mediates M33 desensitization through both receptor phosphorylation and sequestration of GTP-bound $G\alpha_{q/11}$ proteins (Fig. 7*B*). Based on studies with the HCMV-encoded GPCR US28, phosphorylated M33 may interact

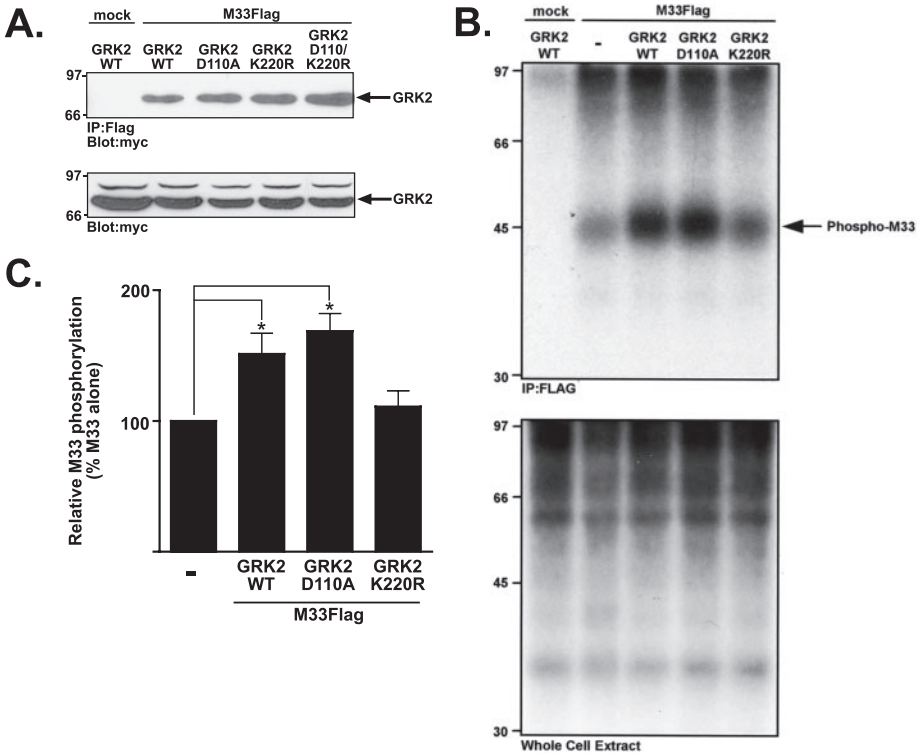

FIGURE 5. **GRK2 interacts with and phosphorylates M33.** *A*, HEK293 cells were transfected with pcDNA3 (mock) or M33FLAG (2 μg) and Myc-tagged WT GRK2, D110A, K220R, or D110A/K220R (2 μg). The cell lysates were incubated with anti-FLAG conjugated agarose beads and immunoblotted for co-immunoprecipitating (*IP*) GRK2 proteins (*upper panel*). Total Myc-tagged GRK2 proteins were detected by immunoblotting transfected cell lysates (*lower panel*). *B*, HEK293 cells transfected with pcDNA3 (mock) or M33FLAG (2 μg) and WT GRK2, D110A, or K220R (2 μg) were radiolabeled with 500 μCi/ml [^{32}P]H_3PO_4 and subjected to an *in vivo* kinase assay. Shown is a representative autoradiograph of four independent experiments (*upper panel*). Whole cell extracts were shown to be similar in ^{32}P incorporation when analyzed by autoradiography (*lower panel*). *C*, M33FLAG basal phosphorylation or phosphorylation in the presence of WT GRK2, D110A, or K220R was quantitated using ImageQuant software. The data represent four independent experiments and are presented as percentages over basal (*, $p < 0.05$).

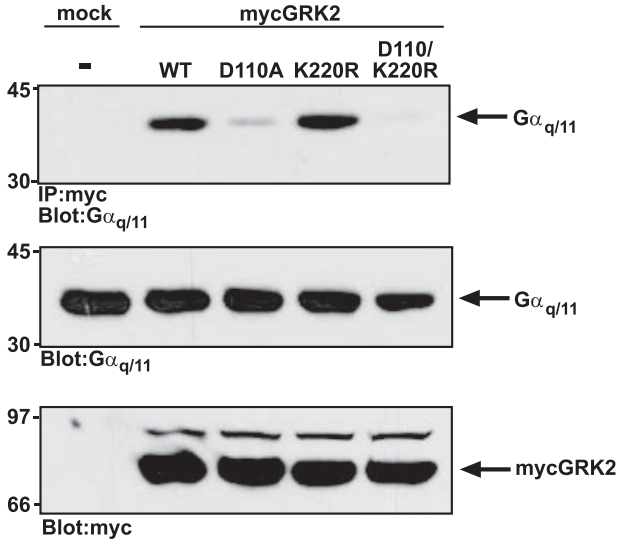

FIGURE 6. **WT GRK2 and K220R, but not D110A or D110A/K220R, bind $G\alpha_{q/11}$.** HEK293 cells were transfected with pcDNA3 (mock) or Myc-tagged WT GRK2, D110A, K220R, D110A/K220R (2 μg) and $G\alpha_{q/11}$ (2 μg). The cell lysates were incubated with anti-Myc-conjugated agarose beads and immunoblotted for co-immunoprecipitating (*IP*) $G\alpha_{q/11}$ (*upper panel*). Total $G\alpha_{q/11}$ (*middle panel*) and total Myc-tagged GRK2 proteins (*lower panel*) were detected by immunoblotting transfected cell lysates with anti-$G\alpha_{q/11}$ or anti-Myc antibodies, respectively.

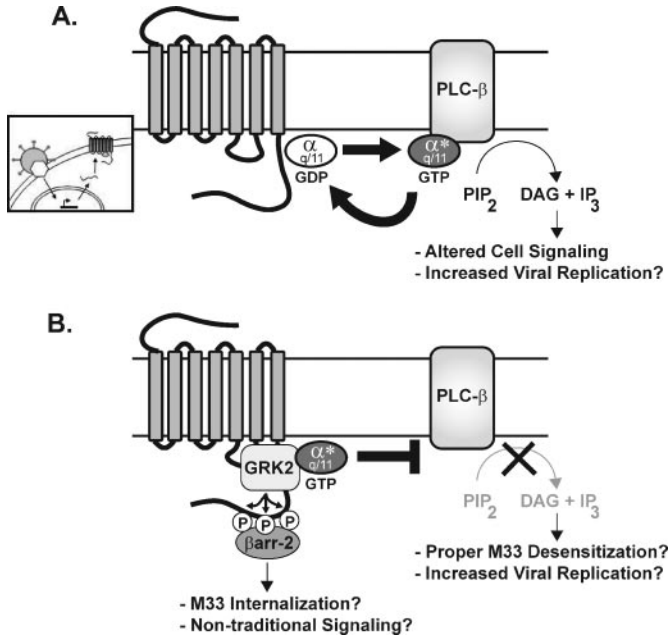

FIGURE 7. **Proposed model of the membrane-proximal events involved in M33 signaling and regulation.** *A*, MCMV infection of a host cell leads to expression of the viral GPCR M33 at the plasma membrane (*inset*). M33 induces high levels of inositol phosphate accumulation in an agonist-independent manner. This is a result of M33 coupling to the $G_{q/11}$ family of heterotrimeric G proteins. *B*, GRK2, a negative regulator of GPCR signaling, effectively desensitizes M33, through both phosphorylation of M33 and sequestration of $G\alpha_{q/11}$ proteins. Phosphorylated M33 may interact with β-arrestin 2, potentially activating non-traditional signaling pathways and promoting M33 internalization in a similar manner to host cell GPCRs.

with β-arrestin 2, potentially activating nontraditional signaling pathways and promoting M33 internalization (47).

DISCUSSION

In this study, we have identified several membrane-proximal events involved in the signaling and desensitization of the MCMV-encoded GPCR M33. Our data indicate that the 10 amino-terminal residues of M33 are required for proper glycosylation patterns as well as membrane localization and subsequent initiation of signal transduction. Moreover, using an R131A point mutant, we have shown that Arg^{131} within the NRY motif of M33 is necessary for M33-induced G protein activation but not interaction.

Through the use of retroviral expression of M33 in WT and $G\alpha_{q/11}$ KO MEFs, we provide genetic evidence to show that M33 directly couples to host cell $G\alpha_{q/11}$ proteins to induce inositol phosphate accumulation. In agreement with previous studies, this coupling occurred in an agonist-independent manner (26). Our data using the genetically altered MEFs are important in that these are the first data that definitively show that a viral seven-transmembrane domain protein utilizes the classical $G_{q/11}$ protein signaling network to induce signaling. Although several viral seven-transmembrane domain proteins had previously been shown to activate classical second messengers such as inositol 1,4,5-triphosphate, prior to our studies it remained possible that the viral proteins may utilize a G protein-independent mechanism to induce second messenger generation.

Desensitization of activated GPCRs by GRKs has largely been seen as an event initiated by GRK phosphorylation of serine and threonine residues within the intracellular loops and carboxyl tail of the receptor. This modality has been reassessed with the growing evidence of phosphorylation-independent regulation of $G_{q/11}$-coupled receptors mediated by the RH domain of GRK2. For example, inositol phosphate accumulation induced by the $G_{q/11}$-coupled H1 histamine receptor was inhibited by wild-type GRK2 or a catalytically inactive K220R mutant yet remained largely unaffected by a D110A/K220R mutant (20). Here, we show that GRK2 regulates M33 signaling and that this regulation requires both the RH domain and kinase domain of GRK2. Furthermore, we show that GRK2, but not a catalytically inactive K220R mutant, enhances basal phosphorylation levels of M33. To our knowledge, this is the first direct evidence demonstrating the function of the RH domain in phosphorylation-independent regulation of a viral GPCR.

Based on the present study, we now appreciate that the similarities between the HCMV GPCR US28 and the MCMV GPCR M33 extend beyond the ability to activate signaling pathways (*e.g.* inositol phosphate accumulation) in an agonist-independent manner. Results from this study indicate that M33, like US28, is regulated by the cellular desensitization machinery including the GRK proteins. GRK2 was shown to dampen US28-induced inositol accumulation through receptor phosphorylation; however, the effect of the GRK2 RH domain was not analyzed (47). Given the similarities between US28 and M33, it is reasonable to suggest that the GRK2 RH domain may also function to suppress US28 signaling independent of receptor phosphorylation. Conversely, the effects of other GRKs may promote M33 desensitization through a phosphorylation-dependent mechanism because another GRK family member, GRK5, was shown to enhance the basal phosphorylation state of US28 (47). The carboxyl tail of M33 is rich in serine and threonine residues (12 amino acids of a predicted 66 total, or 18%), providing multiple potential phosphorylation sites for GRKs or other cellular kinases such as protein kinase C or protein kinase

A. It would be interesting to determine which sites of GRK phosphorylation are necessary for M33 desensitization, as well as examine the effect of other GRKs, specifically GRK5, or cellular kinases on the phosphorylation state of M33.

Regulation of GPCR signaling in general can be viewed as occurring at both the extracellular and intracellular interfaces of the receptor. First, the presence of agonist in the extracellular space and the binding of such are required by most cellular GPCRs. Second, the intracellular desensitization machinery (GRKs and arrestins) functions downstream of agonist binding to attenuate the signaling activity elicited by activated GPCRs. In terms of viral GPCRs, however, the agonist-independent nature of these receptors suggests that the initial extracellular regulation (*i.e.* ligand binding) is circumvented. From a viral perspective, this agonist-independent activity may provide the immediate induction of cell signaling pathways necessary for the success of the virus. However, based on findings in this study as well as in previous reports, viral GPCRs are still subject to intracellular regulation by host cell GRKs and arrestins. Consequently, this intracellular regulation can be viewed as viral "hijacking" of the host cell desensitization machinery and may potentially be necessary to regulate the levels and kinetics to which these receptors signal that are most beneficial to the virus. In this study, the dual mechanism of GRK2 regulation of M33 suggests that M33 signaling activity is tightly regulated, possibly to prevent host cell apoptosis induced by high levels of agonist-independent signaling mediated by M33. Indeed, previous studies have shown that regulation of inositol phosphate formation from the $G_{q/11}$-coupled metabotropic glutamate receptor 1a (mGluR1a) by both WT GRK2 and GRK2 K220R protected cells from mGluR1a-stimulated apoptosis (48). Perhaps MCMV utilizes GRK2 to similarly prevent toxic levels of M33-induced accumulation of second messenger molecules and allow for successful viral replication. Additionally, GRK2 phosphorylation of M33 could trigger a second wave of M33 signal transduction through the recruitment of β-arrestins, which have been shown to activate nontraditional or non-G protein-mediated signaling pathways (49, 50). In support of this hypothesis, initial co-immunoprecipitation studies have suggested that M33 can interact with β-arrestin 2.[3] Future work using a mutant M33 protein lacking carboxyl-terminal serine and threonine residues could address potential anti-apoptotic effects and/or initiation of M33-induced nontraditional signaling pathways resulting from GRK2 phosphorylation.

M33 has been shown to play important roles in viral pathogenesis by promoting cardiovascular smooth muscle cell migration, enabling viral dissemination, and facilitating viral replication within the salivary gland (28, 29). Our data demonstrating that M33 associates with GRK proteins suggest that the GRKs may play an important role in M33 activity *in vivo*. Previous studies have shown that GRK proteins play central roles in cardiovascular disease, and our findings suggest that M33 could potentially augment this disease process by directly interacting with GRK signaling pathways or by sequestering GRK proteins, thus interfering with their ability to regulate cellular GPCRs in the heart. MCMV has been shown to accelerate the development of atherosclerosis in $ApoE^{-/-}$ mice, and it remains to be determined whether M33 and or GRKs are important in this effect of MCMV in the heart (51, 52). Moreover, it is interesting to note that GRK proteins have been reported to regulate chemotaxis, and the ability of M33 to engage this family of cellular regulators may enable cellular migration and/or promote efficient viral dissemination throughout the host (53). A more complete identification of M33 signaling pathways will be important to ascertain what role GRKs may play in M33-directed cell migration.

In conclusion, we have identified a specific G protein-signaling pathway activated by the MCMV GPCR M33. Moreover, the biochemical studies described here demonstrate that the cellular desensitization machinery functions to regulate the signaling activity of M33, providing the basis to examine the role of GRK2-mediated desensitization of M33 in the context of an active viral infection in the host. By extending this work into mouse models of MCMV infection using wild-type and transgenic animals, future studies will elucidate the impact of M33 regulation by GRKs on MCMV pathogenesis *in vivo*.

Acknowledgments—We thank R. Cardin for MCMV-infected cells, R. Sterne-Marr and S. Ferguson for GRK2 constructs, and G. Dorn, II, J. Molkentin, and A. Weiss for critical review of this manuscript. We also thank N. Freedman for helpful discussions.

REFERENCES

1. Fredriksson, R., Lagerstrom, M. C., Lundin, L. G., and Schioth, H. B. (2003) *Mol. Pharmacol.* **63,** 1256–1272
2. Guo, H.-G., Browning, P., Nicholas, J., Hayward, G. S., Tschachler, E., Jiang, Y.-W., Sadowska, M., Raffeld, M., Colombini, S., and Gallo, R. C. (1997) *Virology* **228,** 371–378
3. Ahuja, S. K., and Murphy, P. M. (1993) *J. Biol. Chem.* **268,** 20691–20694
4. Chee, M. S., Satchwell, S. C., Preddie, E., Weston, K. M., and Barrell, B. G. (1990) *Nature* **344,** 774–777
5. Blank, J., Brattain, K., and Exton, J. (1992) *J. Biol. Chem.* **267,** 23069–23075
6. Lee, C., Park, D., Wu, D., Rhee, S., and Simon, M. (1992) *J. Biol. Chem.* **267,** 16044–16047
7. Pitcher, J. A., Freedman, N. J., and Lefkowitz, R. J. (1998) *Annu. Rev. Biochem.* **67,** 653–692
8. Lefkowitz, R. J., and Shenoy, S. K. (2005) *Science* **308,** 512–517
9. Penn, R. B., Pronin, A. N., and Benovic, J. L. (2000) *Trends Cardiovasc. Med.* **10,** 81–89
10. Benovic, J. L., Strasser, R. H., Caron, M. G., and Lefkowitz, R. J. (1986) *Proc. Natl. Acad. Sci. U. S. A.* **83,** 2797–2801
11. DebBurman, S. K., Ptasienski, J., Boetticher, E., Lomasney, J. W., Benovic, J. L., and Hosey, M. M. (1995) *J. Biol. Chem.* **270,** 5742–5747
12. DebBurman, S. K., Ptasienski, J., Benovic, J. L., and Hosey, M. M. (1996) *J. Biol. Chem.* **271,** 22552–22562
13. Pitcher, J. A., Inglese, J., Higgins, J. B., Arriza, J. L., Casey, P. J., Kim, C., Benovic, J. L., Kwatra, M. M., Caron, M. G., and Lefkowitz, R. J. (1992) *Science* **257,** 1264–1267
14. Carman, C. V., Som, T., Kim, C. M., and Benovic, J. L. (1998) *J. Biol. Chem.* **273,** 20308–20316
15. Berman, D. M., Kozasa, T., and Gilman, A. G. (1996) *J. Biol. Chem.* **271,** 27209–27212
16. Hepler, J. R., Berman, D. M., Gilman, A. G., and Kozasa, T. (1997) *Proc. Natl. Acad. Sci. U. S. A.* **94,** 428–432
17. Carman, C. V., Parent, J. L., Day, P. W., Pronin, A. N., Sternweis, P. M., Wedegaertner, P. B., Gilman, A. G., Benovic, J. L., and Kozasa, T. (1999) *J. Biol. Chem.* **274,** 34483–34492
18. Sallese, M., Mariggio, S., D'Urbano, E., Iacovelli, L., and De Blasi, A. (2000) *Mol. Pharmacol.* **57,** 826–831

[3] J. D. Sherrill and W. E. Miller, unpublished data.

19. Dhami, G. K., Dale, L. B., Anborgh, P. H., O'Connor-Halligan, K. E., Sterne-Marr, R., and Ferguson, S. S. G. (2004) *J. Biol. Chem.* **279,** 16614–16620
20. Iwata, K., Luo, J., Penn, R. B., and Benovic, J. L. (2005) *J. Biol. Chem.* **280,** 2197–2204
21. Pass, R. F. (2001) in *Fields Virology* (Knipe, D. M., and Howley, P. M., eds) 4th Ed., Lippincott Williams and Wilkens Publishers, Philadelphia, PA
22. Rosenkilde, M. M., Waldhoer, M., Luttichau, H. R., and Schwartz, T. W. (2001) *Oncogene* **20,** 1582–1593
23. Rigoutsos, I., Novotny, J., Huynh, T., Chin-Bow, S. T., Parida, L., Platt, D., Coleman, D., and Shenk, T. (2003) *J. Virol.* **77,** 4326–4344
24. Rawlinson, W., Farrell, H., and Barrell, B. (1996) *J. Virol.* **70,** 8833–8849
25. Gao, J. L., and Murphy, P. M. (1994) *J. Biol. Chem.* **269,** 28539–28542
26. Waldhoer, M., Kledal, T. N., Farrell, H., and Schwartz, T. W. (2002) *J. Virol.* **76,** 8161–8168
27. Streblow, D. N., Soderberg-Naucler, C., Vieira, J., Smith, P., Wakabayashi, E., Ruchti, F., Mattison, K., Altschuler, Y., and Nelson, J. A. (1999) *Cell* **99,** 511–520
28. Melnychuk, R. M., Smith, P., Kreklywich, C. N., Ruchti, F., Vomaske, J., Hall, L., Loh, L., Nelson, J. A., Orloff, S. L., and Streblow, D. N. (2005) *J. Virol.* **79,** 10788–10795
29. Davis-Poynter, N. J., Lynch, D. M., Vally, H., Shellam, G. R., Rawlinson, W. D., Barrell, B. G., and Farrell, H. E. (1997) *J. Virol.* **71,** 1521–1529
30. Offermanns, S., Zhao, L. P., Gohla, A., Sarosi, I., Simon, M. I., and Wilkie, T. M. (1998) *EMBO J.* **17,** 4304–4312
31. Pear, W. S., Miller, J. P., Xu, L., Pui, J. C., Soffer, B., Quackenbush, R. C., Pendergast, A. M., Bronson, R., Aster, J. C., Scott, M. L., and Baltimore, D. (1998) *Blood* **92,** 3780–3792
32. Paulsen, S. J., Rosenkilde, M. M., Eugen-Olsen, J., and Kledal, T. N. (2005) *J. Virol.* **79,** 536–546
33. Lanctot, P. M., Leclerc, P. C., Clement, M., Auger-Messier, M., Escher, E., Leduc, R., and Guillemette, G. (2005) *Biochem. J.* **390,** 367–376
34. Wess, J. (1997) *FASEB J.* **11,** 346–354
35. Gruijthuijsen, Y. K., Casarosa, P., Kaptein, S. J., Broers, J. L., Leurs, R., Bruggeman, C. A., Smit, M. J., and Vink, C. (2002) *J. Virol.* **76,** 1328–1338
36. Rosenkilde, M. M., Kledal, T. N., and Schwartz, T. W. (2005) *Mol. Pharmacol.* **68,** 11–19
37. Alewijnse, A. E., Timmerman, H., Jacobs, E. H., Smit, M. J., Roovers, E., Cotecchia, S., and Leurs, R. (2000) *Mol. Pharmacol.* **57,** 890–898
38. Gruijthuijsen, Y. K., Beuken, E. V., Smit, M. J., Leurs, R., Bruggeman, C. A., and Vink, C. (2004) *J. Gen. Virol.* **85,** 897–909
39. Bigay, J., Deterre, P., Pfister, C., and Chabre, M. (1985) *FEBS Lett.* **191,** 181–185
40. Paris, S., and Pouyssegur, J. (1987) *J. Biol. Chem.* **262,** 1970–1976
41. Tesmer, V. M., Kawano, T., Shankaranarayanan, A., Kozasa, T., and Tesmer, J. J. (2005) *Science* **310,** 1686–1690
42. Flanagan, C. A. (2005) *Mol. Pharmacol.* **68,** 1–3
43. Dhami, G. K., Anborgh, P. H., Dale, L. B., Sterne-Marr, R., and Ferguson, S. S. G. (2002) *J. Biol. Chem.* **277,** 25266–25272
44. Willets, J. M., Nahorski, S. R., and Challiss, R. A. J. (2005) *J. Biol. Chem.* **280,** 18950–18958
45. Sterne-Marr, R., Tesmer, J. J. G., Day, P. W., Stracquatanio, R. P., Cilente, J.-A. E., O'Connor, K. E., Pronin, A. N., Benovic, J. L., and Wedegaertner, P. B. (2003) *J. Biol. Chem.* **278,** 6050–6058
46. Kong, G., Penn, R., and Benovic, J. (1994) *J. Biol. Chem.* **269,** 13084–13087
47. Miller, W. E., Houtz, D. A., Nelson, C. D., Kolattukudy, P. E., and Lefkowitz, R. J. (2003) *J. Biol. Chem.* **278,** 21663–21671
48. Dale, L. B., Bhattacharya, M., Anborgh, P. H., Murdoch, B., Bhatia, M., Nakanishi, S., and Ferguson, S. S. G. (2000) *J. Biol. Chem.* **275,** 38213–38220
49. Daaka, Y., Luttrell, L. M., Ahn, S., Della Rocca, G. J., Ferguson, S. S. G., Caron, M. G., and Lefkowitz, R. J. (1998) *J. Biol. Chem.* **273,** 685–688
50. Luttrell, L. M., Ferguson, S. S., nbsp, G., Daaka, Y., Miller, W. E., Maudsley, S., Della Rocca, G. J., Lin, F. T., Kawakatsu, H., Owada, K., Luttrell, D. K., Caron, M. G., and Lefkowitz, R. J. (1999) *Science* **283,** 655–661
51. Hsich, E., Zhou, Y. F., Paigen, B., Johnson, T. M., Burnett, M. S., and Epstein, S. E. (2001) *Atherosclerosis* **156,** 23–28
52. Burnett, M. S., Gaydos, C. A., Madico, G. E., Glad, S. M., Paigen, B., Quinn, T. C., and Epstein, S. E. (2001) *J. Infect. Dis.* **183,** 226–231
53. Fong, A. M., Premont, R. T., Richardson, R. M., Yu, Y. R., Lefkowitz, R. J., and Patel, D. D. (2002) *Proc. Natl. Acad. Sci. U. S. A.* **99,** 7478–7483